Volcanic ash in the free atmosphere: A dynamical systems approach

T Haszpra and T Tél

Institute for Theoretical Physics, Eötvös Loránd University, Pázmány Péter sétány 1/A, H-1117 Budapest, Hungary

E-mail: `hatimi@caesar.elte.hu`, `tel@general.elte.hu`

Abstract. The motion of volcanic ash particles is described on large scales by an ordinary differential equation, and the dynamics is chaotic. Deposition with a terminal velocity is found to be influenced by all three components of the wind velocity. The particles sooner or later leave the free atmosphere and enter the planetary boundary layer. Chaos is thus transient, and we point out that quantities like escape rate, average lifetime and topological entropy can efficiently be applied to characterize the volcanic ash dynamics in the free atmosphere. These quantities are evaluated for particular eruption examples of volcano Eyjafjallajökull, as well as for volcanic averages taken at different geographical locations, and for global averages over the Earth.

1. Introduction

The spreading of different forms of air pollutants in the atmosphere is an intensively studied subject (see e.g. [1]). The eruptions of the Iceland's Eyjafjallajökull mid April–mid May 2010, which were relatively weak compared to other volcanic eruptions, called the attention to the particular case of volcanic ash as they caused enormous disruption of air traffic across Europe. In order to characterize the advection and study the dispersion (see e.g., [2, 3]), we apply here a single-particle-approach. Our main aim is to understand the spreading of volcanic ash in the free atmosphere from a dynamical systems point of view (in a different context, see [4]).

It will be demonstrated that the large-scale dynamics can be described by the equations of passive scalar advection in the horizontal direction, but in the vertical direction a well-defined terminal velocity should be taken into account as a term added to the vertical wind velocity. The background wind field data are taken from the ERA-Interim data bank of the European Centre for Medium-Range Weather Forecasts [5].

The simulations show that the advection of volcanic ash is chaotic, but since particles spend a finite period of time in the free atmosphere (before entering the planetary boundary layer, where they become subject to a qualitatively different, noisy dynamics), chaos is transient. We point out that quantities well known from the theory of transient chaos [6] can efficiently be applied to characterize the dynamics of volcanic ash in the free atmosphere. They characterize the deposition as a decay process, the average lifetime outside of the planetary boundary layer, and the stretching rate of material line segments of volcanic ash. We evaluate these measures particular cases of Eyjafjallajökull eruptions, as well as, for global averages taken over several model volcano eruptions distributed over the globe.

The paper is organized as follows. Section 2 gives an overview of the basic equation, of the ECMWF reanalysis wind field and the numerical methods used to determine the trajectories. In Section 3, we present three basic quantities: escape rate, average lifetime, and topological entropy, to be used to characterize the spreading of volcanic ash. The results for local and global averages are presented in Sections 4 and 5, respectively. A summary is given in Section 6.

2. Equations, data and methods

The dynamics of inertial particles in turbulence has attracted recent attention (for a review see [7, 8]). The equations of motion for small, inertial, spherical particles of radius r in a viscous fluid advected by a flow deterministically are given by the Maxey-Riley equations [9, 10]. For heavy particles of density ρ_p much larger than that of the ambient medium ρ, the dimensionless equations for the particles trajectory $\mathbf{r}_p(t)$ read as

$$\ddot{\mathbf{r}}_p = \frac{1}{St}\left(\mathbf{v}(\mathbf{r},t) - \dot{\mathbf{r}}_p - W_{terminal}\mathbf{n}\right), \tag{1}$$

where $\mathbf{v}(\mathbf{r},t)$ is the flow field, $W_{terminal}$ is the dimensionless terminal velocity in still fluid, and $\mathbf{n}$ is a unit vector pointing upwards. Velocity and distance are measured in units of a characteristic velocity U and L, respectively. The Stokes number St appearing here is the dimensionless relaxation time of inertial particles subject to Stokes drag. In a fluid of kinematic viscosity ν, it can be expressed as

$$St = \frac{2r^2\rho_p U}{9\rho\nu L}. \tag{2}$$

Since in the free atmosphere diffusion is negligible on large scales (scales larger than a few 10 kms) [11], Eq. (1) applies to volcanic ash particles if wet deposition and other chemical reactions do not play a role.

It has been observed [12] that the size of typical aerosol particles ranges between $r = 1$ and $r = 12$ μm. Their density is approximately twice as large as that of water. With $\rho_p/\rho = 2000$, $\nu = 10^{-5}$ m^2/s as the kinematic viscosity of air, and a typical large scale atmospheric horizontal distance $L = 1000$ km, the Stokes number is calculated for two typical U values in Table 1, and is found to be very small.

Table 1. Typical smallest and largest Stokes number in the problem.

r [μm]	U [m/s]	St
1	1	$4.44 \cdot 10^{-11}$
12	10	$6.40 \cdot 10^{-08}$

Since the limit of $St \to 0$ in (1) implies finite acceleration only if the paranthesis on the right hand side vanishes, the large-scale equation of motion for aerosol particles becomes even simpler than (1). We conclude that inertial effects are negligible, but in the vertical direction deposition has to be taken into account with a terminal velocity.

The dimensional equation of motion for volcanic ash particles thus follows from (1) as

$$\mathbf{v}_p \equiv \dot{\mathbf{r}}_p = \mathbf{v}(\mathbf{r}_p(t),t) - w_{terminal}\mathbf{n}. \tag{3}$$

The expression for the terminal velocity, from the Stokes law [13], is:

$$w_{terminal} = \frac{2}{9}r^2\frac{\rho_p}{\rho\nu}g. \tag{4}$$

Equation (3) is similar to that used in FLEXPART [14] and NAME [3] but without any stochastic component, and we apply it to different volcanic ash particles, individually. This equation is known to have chaotic solutions for typical velocity fields.

In principle, precise atmospheric trajectories can be determined directly from high resolution wind observations by interpolating between the measuring locations and time instants. In practice, however, trajectory calculations are mostly based on gridded output of numerical models (weather forecasts or reanalyses) such as the ones provided by the European Centre for Medium-Range Weather Forecasts (ECMWF).

In this work, the 3rd generation ECMWF reanalysis ERA-Interim data bank is exploited, which is almost up to date from 01/01/1989 [5]. Zonal (u), meridional (v) and vertical (w) wind velocity components of global geographic coverage are evaluated for the year of 2010. Four values are available each day for 00, 06, 12 and 18 h UTC (Universal Time Coordinated) at each geographic location with a spatial resolution of $1.5° \times 1.5°$ (lat/long). Note that the gridded wind fields are rather smooth, subgrid scale turbulence is not resolved. Although the wind velocity at a given site and time is intended to represent an instantaneous value, direct comparison with high resolution wind tower measurements indicates that the velocity should be regarded as a 6-hour mean value [15].

Global ERA-Interim wind fields are available on 37 pressure levels in the range of 1000–1 hPa [16]. Since we are interested in free atmospheric flow, which takes place above the planetary boundary layer (PBL) (in average above 850 hPa), wind fields were downloaded at pressure levels in the range of 850–100 hPa.

When solving (3), the velocities were interpolated at the particle location (linear in time and in the vertical direction and using bicubic spline interpolation in the horizontal direction). Then the differential equation was solved by using Euler's method with a time step of 45 minutes. We choose $dt = 45$ min, because $dt = 6$ h would lead to unrealistically large displacements of a time step. A decrease of dt from 6 h leads to a change in trajectories and dispersion, but for values smaller than $dt = 45$ min the dispersion of particles does not differ significantly.
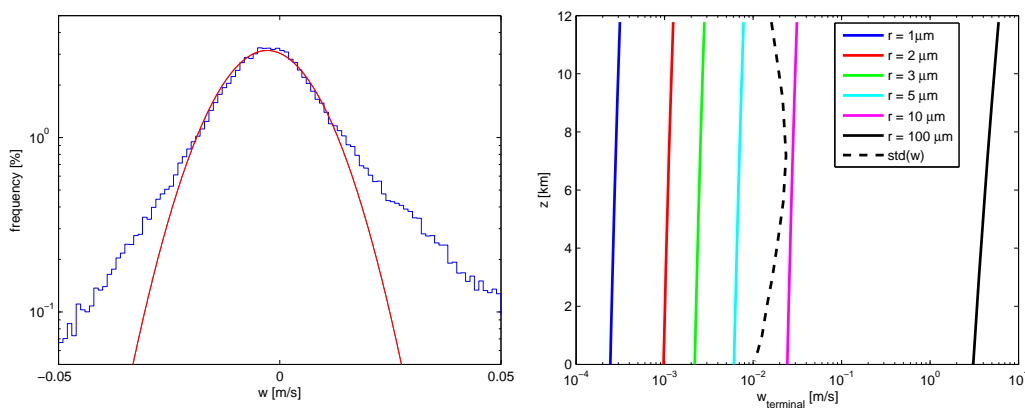
Figure 1. Left panel: Logarithm of the probability distribution of the vertical wind velocity w at 500 hPa on a given day (01.01.2010 at 00, 06, 12, 18 UTC) over the globe. A clear deviation from a Gaussian form (parabola) can be seen with fat tails. Right panel: Terminal velocity $2r^2\rho_p g/(9\rho(z)\nu(z))$ in ICAO standard atmosphere for different particle sizes as a function of height.

Before turning to the results it is worth comparing the histogram of the vertical wind velocity, for example, on the level of 500 hPa (which corresponds approximately to 5.5 km), with the terminal velocity of particles of different sizes in different heights in the ICAO (International Civil Aviation Organization) standard atmosphere [17], we can notice two important features

(Fig. 1). First, the terminal velocity is hardly height-dependent: the decrease in air density appears to be compensated by the increase of the kinematic viscosity due to lower temperatures. Therefore, in (3) we use a constant terminal velocity $\bar{w}_{terminal}$ obtained as an average over height. Second, the magnitude of the standard deviation of the wind velocity fluctuations (black dashed line in the right panel) is larger or is of the same order as the terminal velocity for particles of 1 to 10 μm. Thus, the terminal velocity cannot be assumed to be attained instanteously, and Eq. (3) describes how the vertical wind component influences the deposition dynamics.

Since the downloaded wind data are given in latitude and longitude coordinates on pressure levels, we determined trajectories in the pressure coordinates. The third variable besides the horizontal wind velocity components u and v is the time derivative ω of the pressure coordinate (symbol ω should not be confused with w, that of the vertical wind velocity). The dimension of ω is Pa/s, so the terminal velocity should also be transformed in this variable. For $w_{terminal} > 0$, we expect $\omega_{terminal}$ to be negative. The third component of (3) is

$$\dot{z}_p \equiv w_p = w(\mathbf{r}_p(t), t) - w_{terminal}. \tag{5}$$

Similarly to (5), the vertical equation of motion for a particle in pressure coordinate system is

$$\frac{dp(\mathbf{r}_p(t), t)}{dt} \equiv \omega_p = \omega(\mathbf{r}_p(t), t) - \omega_{terminal}. \tag{6}$$

From the total derivatives we have

$$\omega = \frac{\partial p}{\partial t} + u \frac{\partial p}{\partial x} + v \frac{\partial p}{\partial y} + w \frac{\partial p}{\partial z}, \text{ and } \omega_p = \frac{\partial p}{\partial t} + u_p \frac{\partial p}{\partial x} + v_p \frac{\partial p}{\partial y} + w_p \frac{\partial p}{\partial z}. \tag{7}$$

Since from (3) $u_p = u$ and $v_p = v$, we find that

$$\omega_{terminal} = (w - w_p) \frac{\partial p}{\partial z} = w_{terminal} \frac{\partial p}{\partial z}. \tag{8}$$

If the hydrostatic approximation is valid, i.e., $\partial p / \partial z = -\rho g$, then

$$\omega_{terminal} \approx -\frac{2}{9} r^2 \frac{\rho_p}{\nu} g^2. \tag{9}$$

We have checked that the deviation $(\partial p/\partial z - \rho g)/(\rho g)$ is at most one percent over the full ERA-Interim data bank, which implies that approximation (9) is satisfactory.

As an appropriate choice with the structure of downloaded data, we use spherical coordinates and solve the following equations

$$\frac{d\lambda_p}{dt} = \frac{u(\lambda_p, \varphi_p, p_p, t)}{R_E \cos \varphi_p} , \frac{d\varphi_p}{dt} = \frac{v(\lambda_p, \varphi_p, p_p, t)}{R_E} , \frac{dp_p}{dt} = \omega(\lambda_p, \varphi_p, p_p, t) - \omega_{terminal}, \tag{10}$$

where λ_p and φ_p are the longitude and latitude coordinates of a particle, $p_p(t) \equiv p(\mathbf{r}_p(t), t)$ is the pressure coordinate of a particle, and R_E is the radius of the Earth.

3. Dynamical systems characteristics
Since deposition occurs, volcanic ash particles ultimately reach the planetary boundary layer. Here, however, the character of their equation of motion basically changes due the strong turbulent fluctuations. Within the framework of individual particle simulations turbulence can be taken into account by converting (3) into a stochastic differential equation by adding a noise term of strength proportional to the turbulent eddy diffusivity. The equation is then no longer

determinisic, and the dynamics changes drastically. Here we concentrate on the behaviour in the free atmosphere. Particles are regarded to have escaped from the free atmosphere when entering the boundary layer. Chaotic dynamics is then necessarily of transient character.

A natural quantity characterizing the decaying process is the survival probability, which is proportional to the number $N_p(t)$ of particles staying in the free atmosphere up to time t at least. We consider the lower boundary of the free atmoshpere to be the 850 hPa pressure level. Based on the theory of transient chaos [6], we expect the proportion $N = N_p/N_0$ of non-escaped particles to decay exponentially, i.e.,

$$N(t) \sim \exp(-\kappa t) \tag{11}$$

which is valid after some time. The rate of the decay, called the escape rate, is denoted by κ. It represents the basic escape statistics independent of the initial distribution of the particles. The average lifetime τ of chaos is often estimated as $\tau \sim 1/\kappa$, but this estimate is known to be rather rough. In the knowledge of the particular initial distribution, a direct computation of the average lifetime τ is always useful.

An initially short material line becomes strongly stretched within a short time. The length $L(t)$ of the filament grows rapidly in time and this growth is found to be exponential after some time with an exponent called the topological entropy, h [18]:

$$L(t) \sim \exp(ht). \tag{12}$$

The topological entropy is similar in spirit to, but different in value from the average Lyapunov exponent λ: inequality $h \geq \lambda - \kappa$ should always hold [6]. Our experience shows that the topological entropy is technically much easier to measure than the Lyapunov exponent. When calculating the largest Lyapunov exponent, one selects a reference trajectory and initiates a test particle close to a point of it. When the distance of the pair becomes large enough, one takes another test particle nearby the reference trajectory with an initial distance in the same direction, etc. Since the initial distance cannot be shorter than the grid size, the distance reaches thousands of kilometers within a few days. From the local deviations finite time Lyapunov exponents are obtained which belong, however, to different geographical locations and different times. Averaging them over months provides the value of the average Lyapunov exponent over the entire globe for which we have obtained 0.3 day^{-1} (passive tracers, $r = 0$ μm). We prefer the use of the topological entropy to that of the Lyapunov exponent since even the geographical distribution of the former can be easily obtained as illustrated by Fig. 8.

As characteristic numbers from dynamical system theory, we propose the use of κ, τ and h to measure the dynamics of volcanic ash particles in the free atmosphere. Besides these characteristic numbers, different pictorial representations of the particle cloud are also useful.

4. Local results
We simulated the dispersion of the ash due to the volcanic eruption in Iceland with some simplifications. A single initial column of $1° \times 1° \times 140$ hPa size (~ 100 km $\times$ 100 km $\times$ 4 km) was started at 6 UTC on the 14th of April on the 300 hPa level with $N_0 = 27000$ particles.

The group of charts in Fig. 2 shows the spreading of particles of 10 μm. Due to the relatively large terminal velocity, they are continuously sinking from the initial height of 9 km, and in two days time they reach the level of approximately 600 hPa (the altitude of which is 4.2 km on average). It is also interesting to see in simulations where particles leave the free atmosphere. The last panel shows the location of particles when they reach the upper boundary (850 hPa) of the boundary layer (for the last particles this happens before April 22). The distribution is rather inhomogeneous with strong separation of connected patches, stretching across the width of Siberia. As mentioned simulations were carried out in the free atmosphere, where the effect of
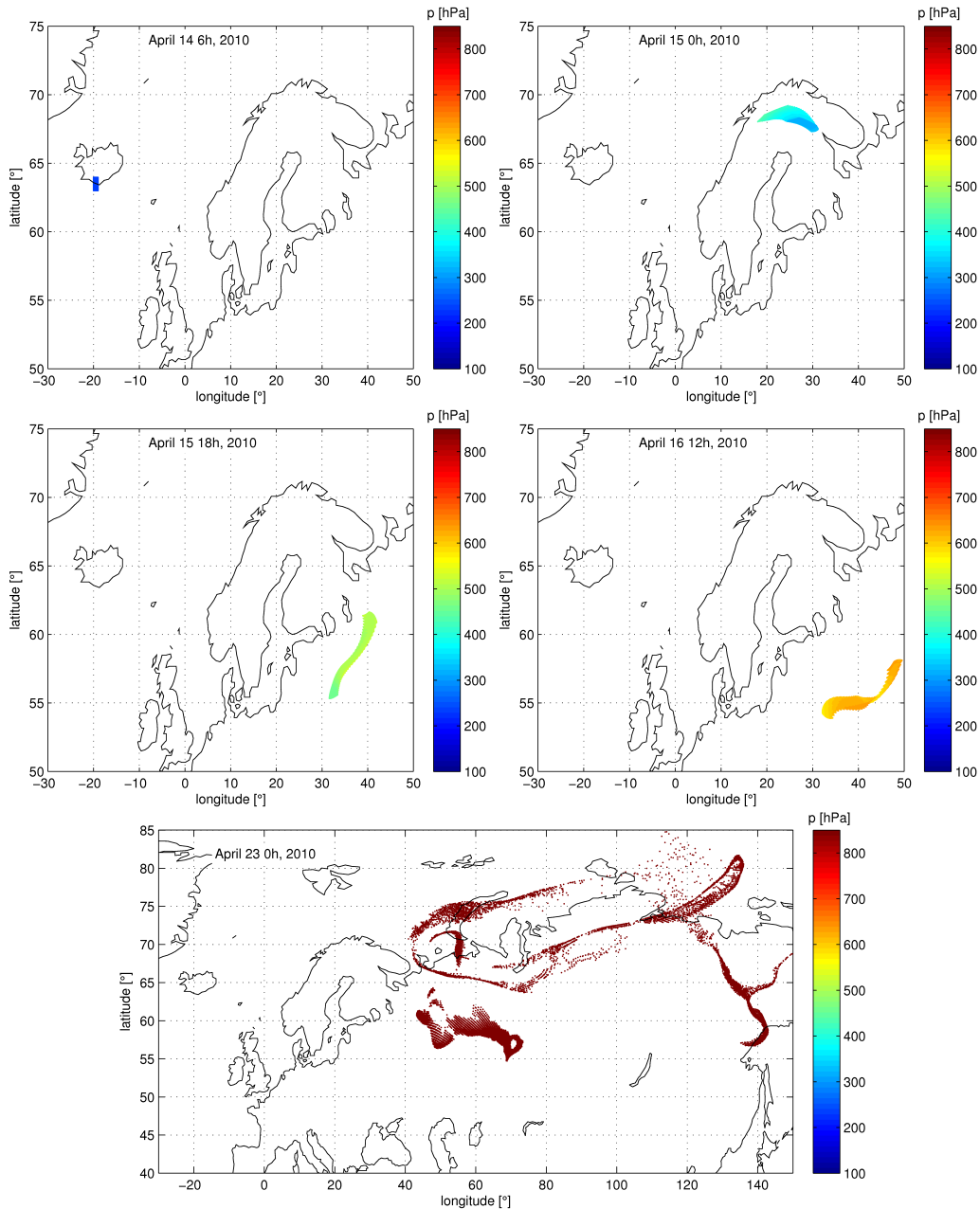
Figure 2. Simulation of the spreading of the volcanic ash ($r = 10\ \mu$m) from Eyjafjallajökull. A single initial column of $1° \times 1° \times 140$ hPa size (~ 100 km $\times$ 100 km $\times$ 4 km) was started at 06 UTC on 14.04.2010 on the 300 hPa level with $N_0 = 27000$ particles. The particular time instants are indicated on the panels.

the turbulent diffusion is known to be negligible: The characteristic scale over which the effect of diffusion can spread in a chaotic flow of average Lyapunov exponent λ is $d = \sqrt{D/\lambda}$ [11]. On scales larger than d, diffusion does not play any role. With $\lambda = 0.3$ day^{-1}, even with a rather large turbulent diffusion coefficient of $D = 10$ m^2/s we obtain $d \sim 2$ km only. We thus conclude that the pattern seen in the free atmosphere (see e.g., Fig. 2) is not influenced at all by diffusion (at most fractality disappears on scales smaller than 2 km, but this horizontal scale is not resolved in any of our large scale distributions). After sinking through the planetary
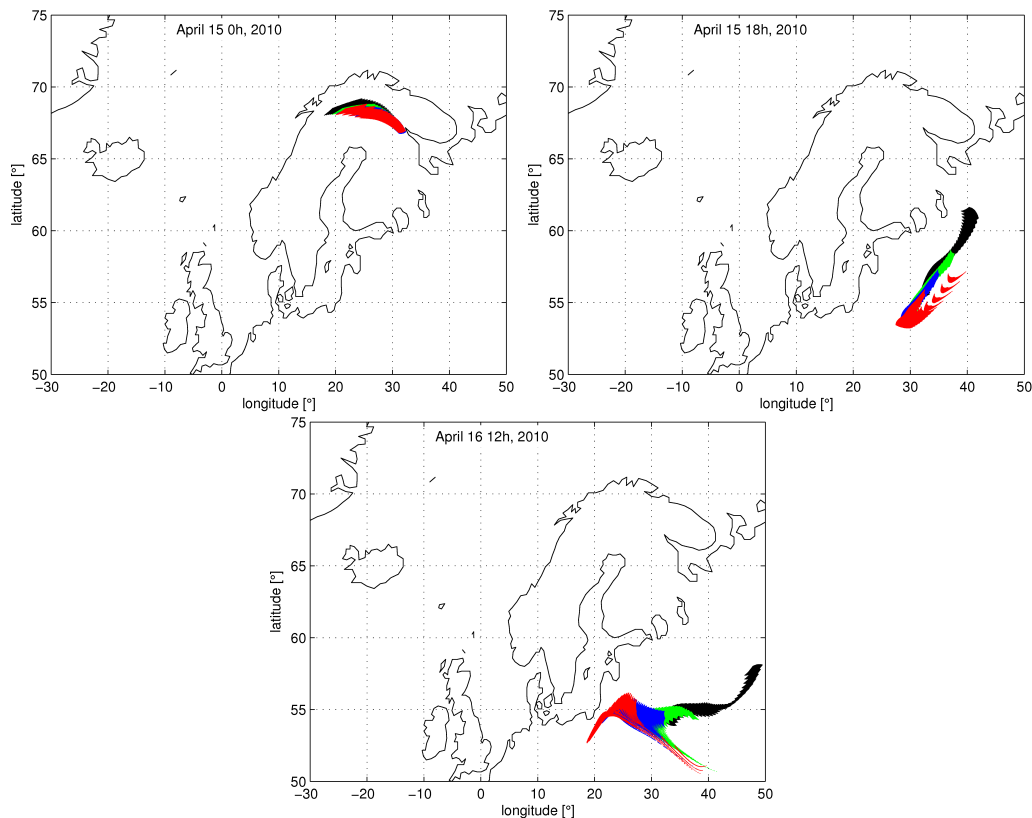
Figure 3. Dispersion of the simulated volcanic ash of different sizes from Eyjafjallajökull (red: $r = 1$ μm, blue: $r = 2$ μm, green: $r = 5$ μm, black: $r = 10$ μm). A single initial column of $1° \times 1° \times 140$ hPa size (~ 100 km $\times$ 100 km $\times$ 4 km) was started at 06 UTC on 14.04.2010 on the 300 hPa level with $N_0 = 27000$ particles. The particular time instants are indicated on the panels.

boundary layer, the true deposition pattern is expected to be qualitatively similar to that seen on the level of 850 hPa.

The group of charts (Fig. 3) illustrates the spreading of particles of different size. A separation can be seen: different types of particles reach different regions being subject to different winds because of their different terminal velocities.

Fig. 4 demonstrates that the particle distribution is wider if another eruption, taking place somewhat later, is also taken into account. The observed total distribution of the volcanic ash on the 16th of April can be seen in the left panel. The accumulation of volcanic ash south of Denmark is apparent in both pictures, but numerical simulation indicates particles in regions further away. Difference might be due to meteorological conditions disturbing satellite observations and to the fact that we only investigated three artificial sudden eruptions, instead of the continuous eruption over the days. In addition, wet deposition was not taken into account.

As Fig. 5 shows, after about 4 days a strong decrease of the survivors takes place. This can be roughly approximated locally by a linear segment in the log-linear representation of the left panel, corresponding to an exponential decay. The approximate value of the escape is found from the range 4.5–8.75 days to be $\kappa = 0.82$ day^{-1}. The average lifetime over the full process is found to be $\tau = 4.86$ day. The a shape of an initially short and straight line of volcanic ash particles becomes quickly stretched and folded as the inset in the right panel shows. The growth rate of the length of this material line is, after about 3 days, clearly exponential (right panel of
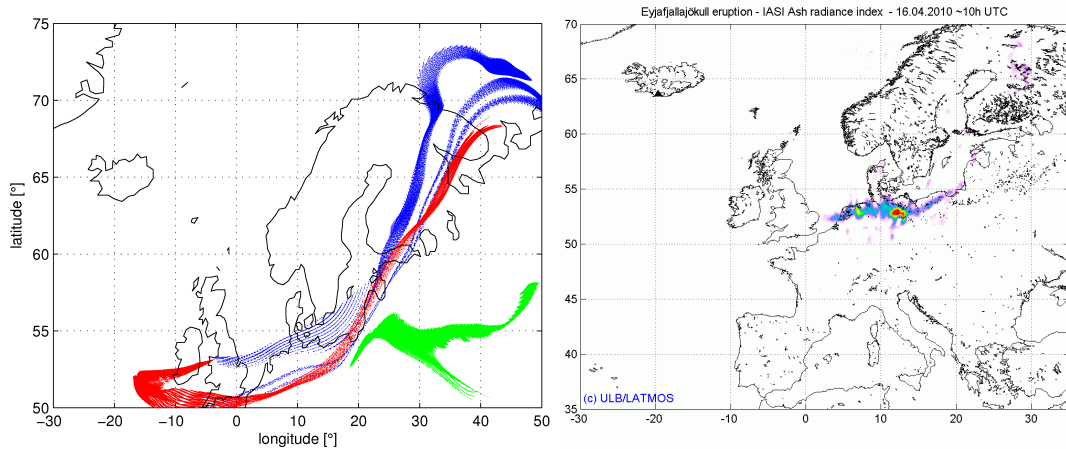
Figure 4. Left panel: Volcanic ash distribution of three model eruptions of Eyjafjallajökull ($r = 1, 2, 5, 10$ μm) at 12 UTC on 16.04.2010. A single initial column of $1° \times 1° \times 140$ hPa size (~ 100 km $\times$ 100 km $\times$ 4 km) was started at 06 (green), 12 (blue) and 18 (red) UTC on 14.04.2010 on the 300 hPa level with $N_0 = 27000$ particles. Right panel: observed volcanic ash distribution at 10 UTC on 16.04.2010 from the homepage of the European Organisation for the Exploitation of Meteorological Satellites (EUMETSAT [19], snapshot taken from a video).

Fig. 5) and a value of $h = 0.68$ day^{-1} follows for this eruption.
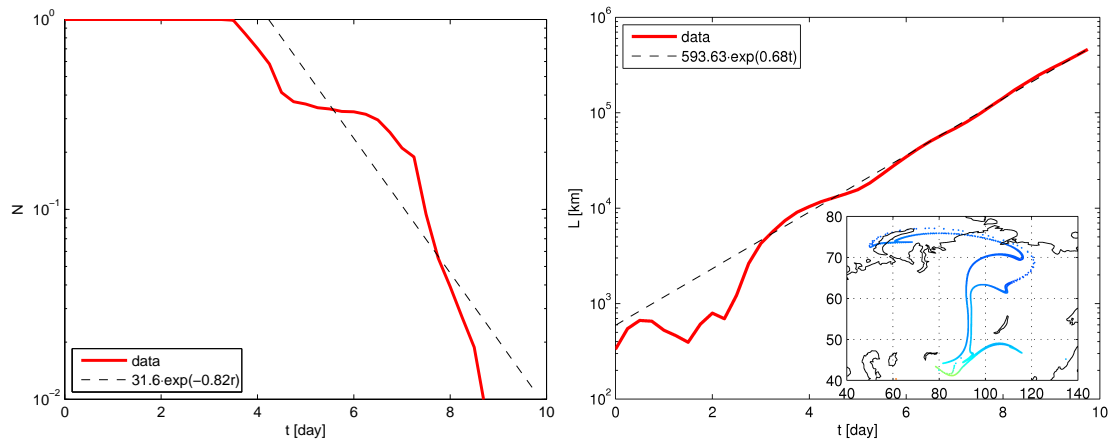
Figure 5. Left panel: The proportion of non-escaped particles as a function of time ($N_0 = 27000$, $r = 10$ μm, $p_0 = 300$ hPa, initial conditions as in Fig. 2). Right panel: the length of a material line of volcanic ash ($L_0 = 3° \approx 330$ km, $N_0 = 10000$, $r = 1$ μm, $p_0 = 300$ hPa) as a function of time. The inset shows the shape of this line at 00 UTC on 20.04.2010.

5. Global results

In order to gain global characteristics of volcanic ash dynamics not related to specific eruptions, we consider several instantaneous model volcanic eruptions distributed over the Globe. Alternatively, we also study an ensemble of a large number of particles distributed uniformly over the Earth at a certain pressure level. In both cases much more precise averages can be obtained (see Fig. 6) then for the particular eruptions on Iceland.

The left panel shows that the number of survivors in the free atmosphere exhibits a clear exponential decay valid over a week or so. By investigating the dependence of the escape rate on the particle radius and the pressure level on which the particles are initially uniformly distributed, we find that $\kappa(r)$ shows a very strong increase with the size (right panel). The escape rate increases by a factor of about 100 between radius 1 and 12 μm. The fit shows that a roughly exponential dependence is found with the size:

$$\kappa(r) \sim \exp(kr), \tag{13}$$

with coefficient $k \approx 0.37$ for any level. Such a strong dependence of the escape rate on a system parameter is found in so-called supertransients occuring in spatio-temporal chaotic models, and in particular in pipe turbulence where this strong dependence on a parameter (the Reynolds number) was also observed in experiments [20].
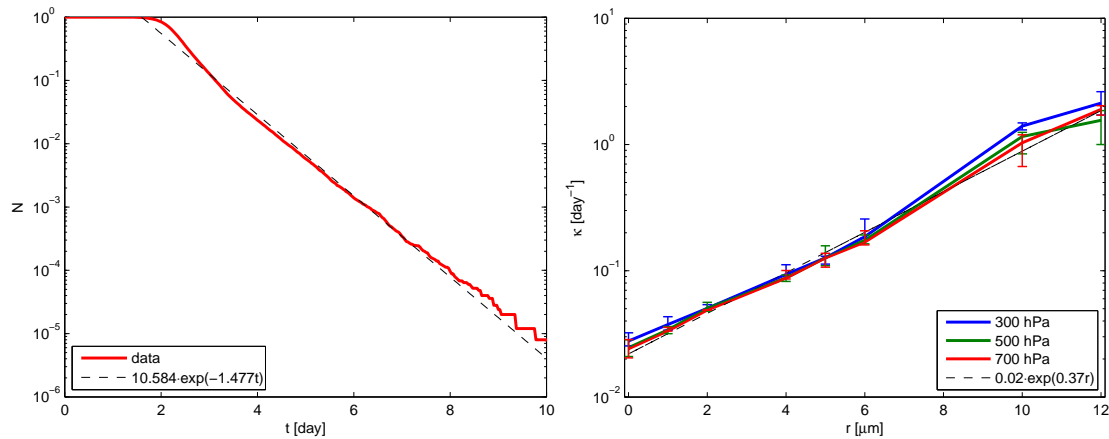
Figure 6. Left panel: The decay of the number of non-escaped particles of radius $r = 10$ μm started from 300 hPa, at 01.01.2010 0 UTC. Right panel: the dependence of the escape rate on size and pressure level. $N_0 = 250000$ particles were distributed uniformly over the whole globe on the level of 300, 500, and 700 hPa. Note that $r = 0$ values are also shown which correspond to the dynamics of air parcels. The non-zero values of the escape rate for $r = 0$ indicate that air parcels also leave the free atmosphere within a finite time.

Concerning the outfall, we estimated the average lifetime (residence time) of particles in two ways. First, as a naive estimate, by using the average terminal velocity of particles between the initial height and the planetary layer's upper boundary in the ICAO standard atmosphere we obtain:

$$\tau_w = \frac{z_{initial} - z_{850hPa}}{\bar{w}_{terminal}}, \tag{14}$$

where $z_{initial} - z_{850hPa} \approx 1560$ m, 4120 m and 7700 m corresponding to the initial level of 700 hPa, 500 hPa and 300 hPa. The results are illustrated by the dotted lines on the different initial levels in Fig. 7. Alternatively, we determined the average lifetime τ from simulations, where 250000 particles were distributed uniformly over the whole globe. For smaller particles enhanced deposition can be observed compared with the naive estimate. The difference is due to the fact that (14) is valid in a continuum at rest, while τ is obtained from solving (3). This shows that the presence of vertical winds is essential for the deposition of volcanic ash, and its role is dominant for small size particles, as also follows from Fig. 1.

The size-dependence is found to be exponential again:

$$\tau(r) \sim \exp(-k'r), \tag{15}$$

9

with $k' \approx 0.30$. The difference between $\tau(r)$ and $1/\kappa(r)$ is due to the fact that with the chosen initial condition all particles spend a long period of time in the free atmosphere, and the decay in the number of survivors starts after a few days only.
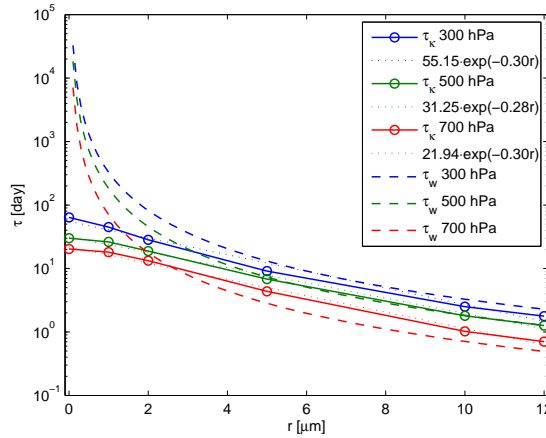

Figure 7. Average residence time τ and the naive estimate τ_w as a function of size and initial pressure level. $N_0 = 250000$ particles were distributed uniformly over the whole globe on the level of 300, 500, and 700 hPa at 01.01.2010 00 UTC.

A detailed investigation of the topological entropy has also been carried out by using several identical short line segments distributed on a grid over the globe initially. Naturally, the topological entropy depends on the actual location implying different meteorological conditions. The topological entropy is found to depend on the initial geographic location, and has mainly zonal distribution (Fig. 8).
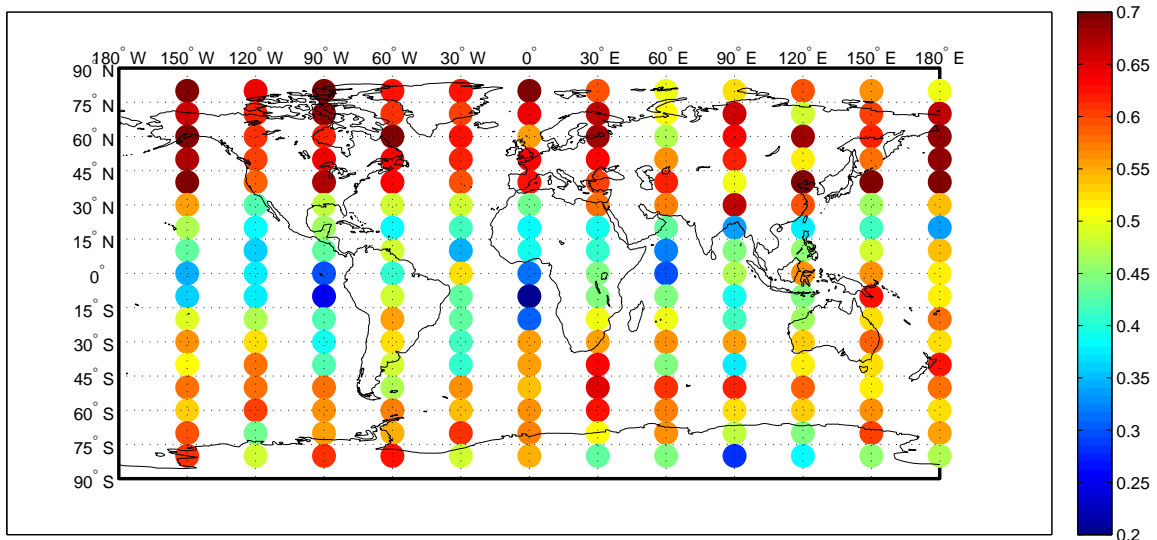
Figure 8. Geographical distribution of the topological entropy obtained from line segments of ash particles of size $r = 1$ μm and of length $3°$ distributed on the 500 hPa level on 01.01.2010 00 UTC which are followed over 10 days.

There are strong differences between the values close to the Equator and in extratropics. The largest values appear in the mid-latitudes (Fig. 9), especially in winter, due to the strong mixing
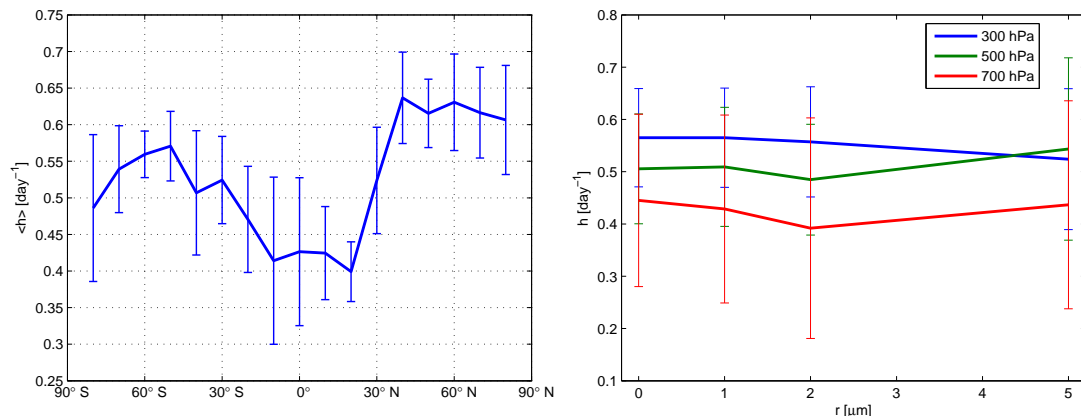
Figure 9. Left panel: zonal average of the topological entropies of Fig. 8 plotted as a function of latitude. Right panel: the dependence of the average topological entropy on particle size and the initial pressure level.

and shearing effects of cyclones on particles, while the smallest values (less than 0.5 1/day) are located in the tropics. Average topological entropy hardly depends on the particle size (Fig. 9). For lines initially started higher in the atmosphere (300 and 500 hPa) the topological entropy is larger than on lower levels.

6. Summary and discussion

In summary, we can say that the advection of volcanic ash is chaotic and particles spend a finite period of time in the free atmosphere. Obviously, the higher the initial height and the smaller the particle, the larger the average life time. An initially localized pollutant cloud becomes strongly stretched in a few days, fine filamentary structures develop and the filaments grow rapidly in time. We demonstrated that transient chaos related quantites like κ, τ, and h are useful characteristics of the statistics of volcanic ash in the free atmosphere.

Because of stretching and folding, the tracers cover almost the whole hemisphere after about a few weeks. Therefore in the future we intend to calculate the encompassing time for small particles, in a similar way as done for air parcels in [21]. Besides this, we plan to estimate the effective fractal dimension of pollutant clouds during the spreading.

In addition, we would also like to study the dispersion in the planetary boundary layer. Here turbulent diffusion plays an important role, and the anisotropy of diffusion, i.e. the difference between horizontal and vertical diffusivities should be taken into account.

References
[1] Stohl A, Huntrieser H, Richter A, Beirle S, Cooper O, Eckhardt S, Forster C, James P, Spichtinger N, Wenig M, Wagner T, Burrows J and Platt U 2003 *Atmos. Chem. and Phys. Disc.* **3** 2101–2141
[2] Leadbetter S J and Hort M C 2011 *J. Volcanol. Geotherm Res.* **199** 2030
[3] Dacre H F, Grant A L M, Hogan R J, Belcher S E, Thomson D J, Devenish B J, Marenco F, Hort M C, Haywood J M, Ansmann A, Mattis I and Clarisse L 2011 *J. Geophys. Res.* (*Preprint* DOI:10.1029/)
[4] Várai A, Vincze M, Lichtenberger J and Jánosi I M 2011 *this volume*

[5] http://www.ecmwf.int/research/era/do/get/era-interim
[6] Lai Y C and Tél T 2011 *Transient Chaos: Complex Dynamics on Finite-Time Scales* (Springer)
[7] Toschi F and Bodenschatz E 2009 *Annu. Rev. Fluid. Mech.* **41** 375
[8] Cartwright J H E, Feudel U, Károlyi G, de Moura A, Piro O and Tél T 2010 *Nonlinear Dynamics and Chaos: Advances and Perspectives* ed Thiel M, Kurths J, Romano M, Károlyi G and de Moura A (Berlin: Springer)
[9] Maxey M R and Riley J J 1983 *Phys. Fluids* **26** 883
[10] Auton T R, Hunt J and Prud'homme M 1988 *J. Fluid. Mech.* 241
[11] Tél T *et al.* 2000 *Chaos* **10** 89
[12] http://cimss.ssec.wisc.edu/goes/blog/wp-content/uploads/2010/04/
[13] Kundu P K and Cohen I M 2008 *Fluid Mechanics* (Academic Press)
[14] Stohl A, Forster C, Frank A, Seibert P and Wotawa G 2005 *Atmos. Chem. Phys.* **5** 2461
[15] Kiss P, Varga L and Jánosi I M 2009 *J. Renewable Sustainable Energy* **1** 033105
[16] http://data-portal.ecmwf.int/data/d/interim_daily/
[17] http://www.atmosculator.com/The Standard Atmosphere.html
[18] Newhouse S E and Pignataro T 1993 *J. Stat. Phys.* **72** 1331
[19] http://www.eumetsat.int/Home/Main/News/Features/717626
[20] Tél T and Lai Y C 2008 *Phys. Rep.* **460** 245
[21] Haszpra T, Kiss P, Tél T, and Jánosi I M 2011 Advection of passive tracers in the atmosphere: Batchelor scaling Submitted to Int. J. Bif. and Chaos